Assessment of peripheral tissue perfusion by optical dynamic fluorescence imaging and nonlinear regression modeling

Yujung Kang*[a], Jungsul Lee*[a], Kihwan Kwon[b], Chulhee Choi[a,c,d]

[a]Department of Bio and Brain Engineering, KAIST, Daejeon, Korea 305-751;

[b]Department of Cardiology, College of Medicine, Ewha Womans University, Seoul, Korea 158-710;

[c]Graduate School of Medical Science and Engineering, KAIST, Daejeon, Korea 305-751;

[d]KAIST Institute for the BioCentury, KAIST, Daejeon, Korea 305-751

Author for correspondence: Chulhee Choi, Department of Bio and Brain Engineering, Graduate School of Medical Science and Engineering, and KI for the BioCentury, KAIST, Daejeon 305-751, Korea. Fax: 82-42-869-4380; Tel: 82-42-869-4321; E-mail: cchoi@kaist.ac.kr

*These authors contributed equally to this work.

ABSTRACT

The purpose of this study is to examine the peripheral tissue perfusion rates by time-series analysis of distribution and elimination kinetics of a clinically proven NIR fluorescence probe, indocyanine green (ICG). We developed a new method, dynamic ICG perfusion imaging technique to evaluate peripheral tissue perfusion that employs planar imaging with a CCD digital imaging system and time-series analysis of the spatiotemporal

Photonic Therapeutics and Diagnostics VI, edited by N. Kollias, B. Choi, H. Zeng, R. S. Malek, B. J.-F. Wong, J. F. R. Ilgner, K. W. Gregory, G. J. Tearney, L. Marcu, H. Hirschberg, S. J. Madsen, A. Mandelis, A. Mahadevan-Jansen, E. D. Jansen, Proc. of SPIE Vol. 7548, 75483L · © 2010 SPIE · CCC code: 1605-7422/10/$18 · doi: 10.1117/12.841620

dynamics (150s) of intravenously injected ICG by using nonlinear regression and differential evolution methods. Six parameters (α, β, s, d, m; parameters which depend on an arterial input function (AIF) into a lower extremity and p; perfusion rates in the lower extremity) were estimated by the nonlinear regression modeling method. We have confirmed the validity of our new method by applying the method to a normal control and a patient with peripheral arterial occlusion disease (PAOD). PAOD patient showed a unique AIF curve pattern, which was caused by collateral blood flow bypassing the occluded major artery. The lower extremity tissue perfusion rate of the PAOD patient was estimated as about 35% of those of normal values. These results indicate that ICG perfusion imaging method is sensitive enough to diagnose PAOD and capable of diagnosing functional arterial diseases.

Keyword: Indicator dilution curve, mathematical modeling, non-linear regression, differential evolution, peripheral arterial occlusive disease, tissue perfusion, NIR fluorescence imaging.

1 INTRODUCTION

Although peripheral vascular disease (PVD) is prevalent in the primary care setting, it has also been unrecognized and undertreated.[1] Diagnostic methods presently used include the ankle brachial index (ABI), Doppler ultrasonography, plethysmography, and angiography by X-ray or computed tomography (CT), all of which have limitations.[1, 2] Diagnostic modality to assess functional tissue perfusion will be ideal for the periodic checkup, early diagnosis, and adequate treatment of PVD.

Indicator dilution methods have clinical and experimental potential as tools for measuring physiological circulatory parameters such as tissue perfusion because they can be used to provide estimates of blood flow and volumes of the intra and extravascular space.[3-6] The techniques rely on an intravenous bolus administration of a tracer at a specific site of the circulatory system, followed by frequent blood sampling or time-series imaging noninvasively at a distal site. However, concentration-time profile contained re-circulatory information which distorts the downslope of the observed curve. To analyze this recursive curve, various approaches such as

extrapolation,[5] deconvolution[7] or partial differential equation (PDE)[3] or fitting of the curve with gamma,[8] lognormal[9] and local density random walk probability distributions[8, 10] have been studied. Even though these methods were suggested as novel approach for estimation of the pulmonary circulation,[6] cardiac output according to the systemic vascular resistance[4], blood volume,[3, 5] mean transit time,[11] previous studies were not applied for diagnosis of vascular diseases.

We have developed an ICG perfusion imaging method that employs intravenously injected near infrared (NIR) contrast media, indocyanine green (ICG) and time-series planar NIR fluorescence imaging to assess perfusion in the lower extremities based on the animal studies.[12] Although, ICG perfusion imaging could be successfully applied to the clinical trial,[13] there were several differences in probe pharmacokinetics between the mouse and human. In this study, we present a novel modeling approach using nonlinear regression and differential evolution method for measurement of tissue perfusion and arterial input function (AIF) in the human lower extremity. Moreover, we have validated this modeling by applying the method to a normal control and a patient with peripheral arterial occlusion disease (PAOD).

2 METHODS and MATHEMATICAL MODELING

2.1 Subjects

All protocol, survey, and consent forms were approved by the Institutional Review Board of Ewha Womans University Mokdong Hospital. Written informed consent was obtained from subjects. A 61-year old woman was recruited as healthy subject who was non-smoker and manifested no symptoms of lower extremities. A 70-year old man with mild claudication was recruited as a patient with PAOD. He had also diagnosed with type 2 diabetes mellitus 4 years ago. His blood glucose level was higher (168 mg/dl) than healthy subject (87 mg/dl), and he has been treated with glimepiride without insulin therapy. To evaluate the time-series ICG perfusion imaging as a reliable tool for diagnosis of PAOD, we performed also CT-angiography and ABI.

2.2 Diagnosis of PAOD

2.2.1 NIR Fluorescence Imaging

An ICG fluorescence imaging system for lower extremities has been developed by Vieworks Corporation (Seongnam, Gyeonggi-do, Korea).[13] This imaging system employed a CCD digital camera with a 830nm band-pass filter and 760nm light emitting diode arrays. After remaining supine for 5–10 min, 30 serial images (748 × 518 pixels) of both feet were taken at 5-s intervals for 200 s immediately after an intravenous bolus injection of ICG (0.16 mg/kg) for obtaining indicator dilution of ICG fluorescence. This ICG dilution curve was translated into quantitative tissue perfusion and AIF using followed mathematical modeling.

2.2.2 CT-Angiography

CT angiography was performed with a 16-MDCT scanner (SOMATOM Sensation; Siemens Medical Solutions, Erlangen, Germany). An 18-gauge catheter was placed into the antecubital vein, and 120 ml of nonionic contrast material (Iohexol, Omnipaque 300, Nycomed; Amersham, Princeton, UK) was injected at 4 ml/s. CT scans were obtained from above the iliac bifurcation to the feet. Postprocessing for CT angiography resulted in images rotated over 360° for the aortoiliac, femoropopliteal, and tibial arteries using commercially available cardiac reconstruction software (Syngo, version A50A; Siemens Medical Solutions).

2.2.3 ABI

After remaining supine for 5–10 min, blood pressures were recorded in both brachial arteries and in the dorsalis pedis and posterior tibial arteries (VasoGuard P84; SciMed Ltd., Bristol, UK). The ABI was calculated for each leg by dividing the highest ankle systolic pressure by the highest brachial systolic pressure.

2.3 Model Based Analysis of the ICG Dilution Curve

2.3.1 Non Linear Regression Model.

To translate the ICG dilution curve into quantitative tissue perfusion in lower extremity, perfusion rate (%/min) was defined as the fraction of blood exchanged in the vascular volume of the region of interest (ROI) per minute. We assumed that blood volume through the vasculature in the ROI is time invariant during the imaging, therefore, volumetric inflow and outflow were thought to be the same as the previous report.[12] ROI usually contained several hundred pixels which are unit that we can get the ICG dilution curve from. Therefore,

representative average ICG dilution curve from the ROI is used for evaluating the perfusion rate of the ROI. In the ROI, arterial input function (AIF) of blood has been described as a linear combination of Gaussian functions because the ICG dilution curves registered from the carotid artery[5], iliac artery[6] and large peripheral artery[3] show two major peaks which indicates first and second circulation.

$$AIF(t) = \sum_{k=0}^{r-1} d^{\mathrm{k}} \exp\left(-\alpha s^{\mathrm{k}+1}\left(t - (\beta + \mathrm{k}m)\right)^2\right) \tag{1}$$

where r is number of observable circulatory peak, we used 2 for *r* to consider up to second recirculation. *α* determines sharpness of the first peak, *s* determines broadening of the second peak from the first one and *β* is the time-to-peak (sec) in the first peak after appearance of the first fluorescence signal. Parameter *m* is interval (sec) of time-to-peak between first and second peak, and *d* is height ratio of the second to first peak (Figure 1).

The change of ICG concentration of the ROI can be described using Fick's law:

$$\{\text{change of the concentration}\} = \{\text{inflow}\} - \{\text{outflow}\}$$

$$\mathrm{I'_{ROI}} = p \cdot \mathrm{AIF} - p \cdot \mathrm{I_{ROI}} \tag{2}$$

where $\mathrm{I_{ROI}}$ is ICG fluorescence intensity observed in the ROI. Because we assume that the ICG concentration in the ROI is homogenous, the ICG concentration of the outflow is the same as that of the ROI. *p* represents perfusion rate of the ROI. By solving Equation 2 with Laplace transformation, we get $\mathrm{I_{ROI}}$ as a convolution of AIF and exponential decay as follows using Equation 3:

$$\mathrm{I_{ROI}}(\mathrm{t}) = p(\exp(-p\mathrm{t}) * \mathrm{AIF}(\mathrm{t})) \tag{3}$$

$$\mathrm{I_{ROI}}(\mathrm{t}) = p\left(\exp(-p\mathrm{t}) * \sum_{k=0}^{r-1} \mathrm{d}^{\mathrm{k}} \exp\left(-\alpha \mathrm{s}^{\mathrm{k}+1}\left(t - (\beta + \mathrm{km})\right)^2\right)\right) \tag{4}$$

By introducing Equation 1 into Equation 3, exact form of $\mathrm{I_{ROI}}$ could be derived as in Equation 4. *t* indicates time after onset of the fluorescence signal in the ROI.

2.3.2 Differential Evolution

To estimate parameters *α, β, d, m, p,* and *s* in Equation 4, we used differential evolution which had been successfully applied for the evolutionary optimization method over continuous spaces.[14, 15] Briefly, each vector of parameters in initial parameter population is uniformly distributed in predefined range of parameters. Differential evolution generates new parameter vectors by adding a weighted difference vector between two

population members to a third member. In this study, evolution constraint of each generation is the maximum root-mean-square-deviation (RMSD) between experimentally observed average representative ICG dilution curve and numerically estimated ICG dilution curve ($I_{ROI}(t)$) with parameters of each member in population of the immediate previous generation. If the resulting vector yields a smaller RMSD than a constraint, the newly generated vector will replace the vector. If RMSD from population is no smaller than that from the previous generation, evolution terminates. The parameters from last generation are applied to obtain both AIF and perfusion rate of ROI. Imaging processing and data analysis were performed using Visual C^{++} (version 4.0; Microsoft, Redmond, WA, USA).

3 RESULTS

3.1 Diagnostic Results of the CT angiography and ABI

A healthy subject had normal ABI values, 1.08 on the left side and 1.03 on the right side and showed no abnormality in the lower extremity CT angiography (Figure 3A). In contrast, the patient with PAOD had abnormal ABI values, 0.7 on the left side and non-detectable level on the right side. CT-angiography of lower extremity revealed occlusion at right external iliac artery, proximal and mid-portion of superficial femoral artery and left proximal superficial femoral artery with well-developed collateral vessels on left and right superficial femoral arteries and also multiple calcifications on the right and left major arteries as bright white lumps (Figure 4A).

3.1 Estimation of the Tissue Perfusion Based on the Non-Linear Regression Modeling

For measurement of the perfusion rate, ROI was obtained in and around toenails where both arterial inflow through major arteries and circulation through capillaries could be represented strongly compared to the other regions of foot where venous circulation was represented dominantly from. Therefore ICG dilution curves in and around toenails showed shorter time-to-peak and higher maximal intensity than ones in the other regions. The average representative ICG dilution curves from feet of the healthy subject showed rapid time-to-peaks of around 10 sec after onset time of fluorescence signal and precipitous down-slope (Figure 2). In contrast, the

average representative ICG dilution curves from feet of the PAOD patient showed remarkably delayed time-to-peaks of around 45 to 75 sec after onset time of fluorescence signal and no down-slope within 150 sec after onset time. Because the difference of the ICG dilution curve is dependent on tissue perfusion,[12, 13, 16] based on the Equation 4, ICG dilution curves were translated into the quantitative perfusion rates and AIFs (Figure 3B, C and 4B, C). The feet perfusion rates of the healthy subject were 51.4 and 64.2 %/min and the perfusion rates of the PAOD patient were 21.3 and 17.7 %/min, which are about 27 to 41 % of the normal perfusion rates. Estimated AIF of the healthy subject showed separate two peaks with average 96.5 sec interval (m) and 0.1 intensity ratio of the second peak to the first peak (d). In contrast, two peaks in the estimated AIF of the PAOD patient were not separated over time which showed m as average 13.52 sec and d as 1.0. In the estimated AIFs, α, sharpness of the first peaks of the healthy subject were 11.8 and 12.5 from Lt. and Rt., respectively which were similar or relatively small compared to the those of PAOD patient (22.1 and 11.7) and β, the time-to-peaks of first peak of the healthy subject (11.8 and 12.3 sec) was relatively short compared to β of PAOD patient (22.1 and 13.7 sec).

4 DISCUSSIONS

We have previously developed a novel ICG perfusion imaging method that employs the intravenous injection of ICG dye, time-series planar imaging with a CCD digital imaging system, and analysis of ICG dilution curve using mathematical modeling.[12, 13] In this study, we further demonstrated the advantage of the novel modeling approach with nonlinear regression and differential evolution methods for clinical application of ICG perfusion imaging.

Although methods for measuring functional tissue perfusion in the peripheral tissue are required for validation of our novel imaging method, there is no comparable method for measuring functional tissue perfusion especially in the peripheral tissues. Therefore, we compared the perfusion rates and AIFs evaluated from volunteers with lower extremity CT-angiography and ABI which revealed large arterial occlusions. The perfusion rates showed positive correlation with lower extremity CT-angiogram and ABI, even though more extensive clinical data are still needed.

The ABI test is known to be highly sensitive and specific for diagnosing PAOD in patients with severe arterial stenosis; however, it is also known to be unreliable on patients with arterial calcification which results in less or incompressible arteries.[1, 17] Because the stiff arteries produce falsely elevated ankle pressure, false negative results are often found in patients with diabetes mellitus, renal failure or heavy smoker.[18-20] In this study, ABI value even was not detected on the right side of the PAOD patient with multiple calcification in lower extremities. On the other hand, the perfusion rate of this foot was quantitatively estimated by the ICG perfusion imaging. Therefore, we believe that the ICG perfusion imaging can diagnose the perfusion rate in the foot even with stiff arteries due to the calcification and therefore it can be applied to patients with diabetes mellitus as well as PAOD.

AIF as well as perfusion rate is evaluated simultaneously from the ICG dilution curve. To express recirculation pattern, AIF has been modeled to have two peaks within 150 sec after onset of ICG fluorescence signal in the ROI. Because the plasma ICG is rapidly eliminated with a half-life of about 3-4 min by enterohepatic route,[21] if the second peak was due to the recirculation, the intensity ratio of second to first peak should be remarkably smaller and there should be enough interval time between two peaks. In the estimated AIF, second peak in the healthy subject could represent recirculation; however, in PAOD patient, the second peak might be supposed as another blood flow through collaterals because of high intensity ratio and too small interval to be considered to be recirculation. CT-angiogram also shows well-developed collaterals to support this idea. These remarkable differences of the AIFs between a healthy and a PAOD patient might provide information about functional tissue perfusion along with perfusion rate, especially in the case of the patient with chronic occlusive disease and gradual collateralization. Nonetheless, the large-scale clinical studies are necessary to get a conviction of this result.

5 CONCLUSIONS

ICG perfusion imaging has multiple advantages such as superior sensitivity,[12] cost-effectiveness and minimal invasiveness. Even though this study enrolled only two subjects for validation of novel mathematical modeling, the results clearly suggest that the ICG perfusion imaging based on this novel modeling could be reliable

method for diagnosis of PAOD.

ACKNOWLEDGEMENT

This work was supported by the Korea Healthcare Technology R&D Project (A091258), Ministry for Health, Welfare and Family Affairs of the Republic of Korea.

REFERENCE

[1] Stein, R., Hriljac, I., Halperin, J. L., Gustavson, S. M., Teodorescu, V. and Olin, J. W., "Limitation of the resting ankle-brachial index in symptomatic patients with peripheral arterial disease," Vascular medicine 11(1), 29-33 (2006)

[2] Kramer, C. M., "Peripheral arterial disease assessment: wall, perfusion, and spectroscopy," Top Magn Reson Imaging 18(5), 357-369 (2007)

[3] Karalis, V., Dokoumetzidis, A. and Macheras, P., "A physiologically based approach for the estimation of recirculatory parameters," The Journal of pharmacology and experimental therapeutics 308(1), 198-205 (2004)

[4] Krejcie, T. C., Wang, Z. and Avram, M. J., "Drug-induced hemodynamic perturbations alter the disposition of markers of blood volume, extracellular fluid, and total body water," The Journal of pharmacology and experimental therapeutics 296(3), 922-930 (2001)

[5] Picker, O., Wietasch, G., Scheeren, T. W. and Arndt, J. O., "Determination of total blood volume by indicator dilution: a comparison of mean transit time and mass conservation principle," Intensive care medicine 27(4), 767-774 (2001)

[6] Weiss, M., Krejcie, T. C. and Avram, M. J., "Transit time dispersion in pulmonary and systemic circulation: effects of cardiac output and solute diffusivity," American journal of physiology 291(2), H861-870 (2006)

[7] Wittsack, H. J., Wohlschlager, A. M., Ritzl, E. K., Kleiser, R., Cohnen, M., Seitz, R. J. and Modder, U., "CT-perfusion imaging of the human brain: advanced deconvolution analysis using circulant singular value

decomposition," Comput Med Imaging Graph 32(1), 67-77 (2008)

[8] Mischi, M., den Boer, J. A. and Korsten, H. H., "On the physical and stochastic representation of an indicator dilution curve as a gamma variate," Physiological measurement 29(3), 281-294 (2008)

[9] Band, D. M., Linton, R. A., O'Brien, T. K., Jonas, M. M. and Linton, N. W., "The shape of indicator dilution curves used for cardiac output measurement in man," The Journal of physiology 498 (1), 225-229 (1997)

[10] Mischi, M., Kalker, T. A. and Korsten, E. H., "Contrast echocardiography for pulmonary blood volume quantification," T-UFFC 51(9), 1137-1147 (2004)

[11] Sparacino, G., Bonadonna, R., Steinberg, H., Baron, A. and Cobelli, C., "Estimation of organ transport function for recirculating indicator dilution curves," Annals of biomedical engineering 26(1), 128-137 (1998)

[12] Kang, Y., Choi, M., Lee, J., Koh, G. Y., Kwon, K. and Choi, C., "Quantitative analysis of peripheral tissue perfusion using spatiotemporal molecular dynamics," PLoS ONE 4(1), e4275 (2009)

[13] Kang, Y., Lee, J., Kwon, K. and Choi, C., "Application of novel dynamic optical imaging for evaluation of peripheral tissue perfusion," International journal of cardiology doi:10.1016/j.ijcard.2008.12.166, (2009)

[14] Ilonen, J., Kamarainen, J. and Lampinen, J., "Differential Evolution Training Algorithm for Feed-Forward Neural Networks," Neural Processing Letters 17, 93-105 (2003)

[15] Storn, R. and Price, K. V., "Differential evolution-a simple and efficient heuristic for global optimization over continuous spaces," Journal of Global Optimization 11, 341-359 (1997)

[16] Abels, C., "Targeting of the vascular system of solid tumours by photodynamic therapy (PDT)," Photochem Photobiol Sci 3(8), 765-771 (2004)

[17] Allison, M. A., Hiatt, W. R., Hirsch, A. T., Coll, J. R. and Criqui, M. H., "A high ankle-brachial index is associated with increased cardiovascular disease morbidity and lower quality of life," Journal of the American College of Cardiology 51(13), 1292-1298 (2008)

[18] American Diabetes Association, "Peripheral arterial disease in people with diabetes," Diabetes care 26(12), 3333-3341 (2003)

[19] Aboyans, V., Ho, E., Denenberg, J. O., Ho, L. A., Natarajan, L. and Criqui, M. H., "The association between elevated ankle systolic pressures and peripheral occlusive arterial disease in diabetic and nondiabetic subjects," J Vasc Surg 48(5), 1197-1203 (2008)

[20] Novo, S., "Classification, epidemiology, risk factors, and natural history of peripheral arterial disease," Diabetes obesity and metabolism 4(2), S1-6 (2002)

[21] Bollinger, A., Saesseli, B., Hoffmann, U. and Franzeck, U. K., "Intravital detection of skin capillary aneurysms by videomicroscopy with indocyanine green in patients with progressive systemic sclerosis and related disorders," Circulation 83(2), 546-551 (1991)

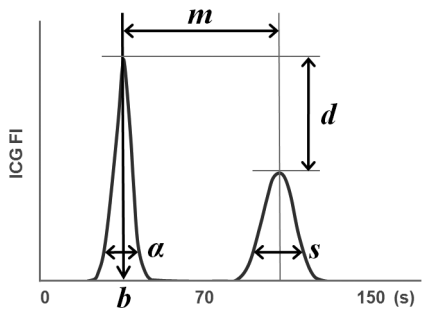

Figure 1. Diagram of the AIF and parameters. The typical AIF into the ROI has two peaks.

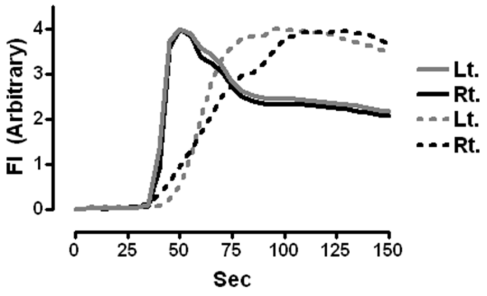

Figure 2. Representative ICG dilution curve. The solid and dotted lines indicate ICG dilution curve of the healthy subject and the patient with PAOD, respectively. X-axis represents time after ICG injection.

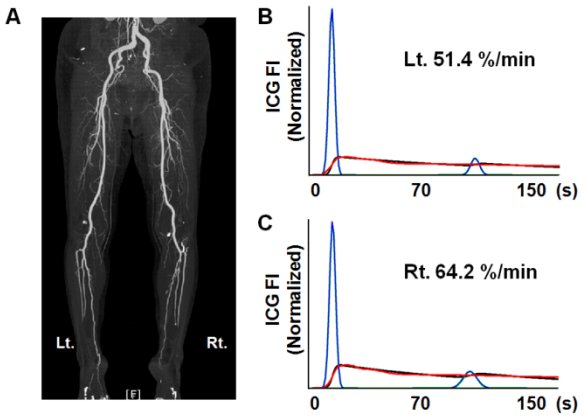

Figure 3. A 61-year-old healthy subject. A. lower extremity CT-angiography. B, C. X- and y-axis indicate time after onset of ICG fluorescence signal from the ROI and ICG fluorescence intensity (FI), respectively. Red line indicates ICG dilution curve obtained from real data while the modeled curve fitted to the real ICG dilution curve by differential evolution is indicated as black line. Estimated AIF shows typical separated two peaks (green line). Summed kinetics of the two peaks is indicated by blue line from the Left (B) and Right (C) foot. The number within the graph shows perfusion rate. Red and black line show ICG FI value amplified as 3-fold to visualize well. Green and blue line overlap completely because two peaks are separated perfectly.

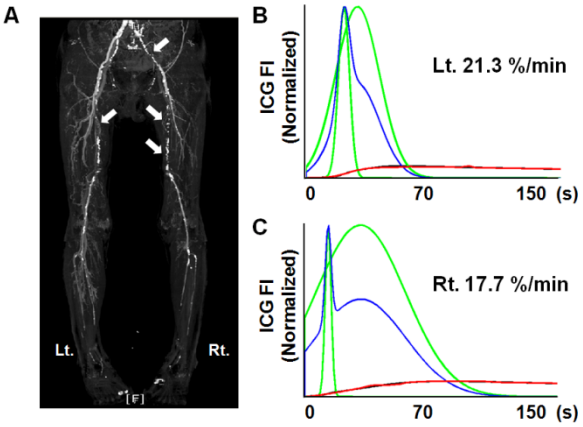

Figure 4. A 70-year-old patient with PAOD. A. lower extremity CT-angiography. Arrows indicate arterial occlusive regions. B, C. X- and y-axis indicate time after onset of ICG fluorescence signal from the ROI and ICG fluorescence intensity (FI), respectively. ICG dilution curve (red line), curve fitted to the ICG dilution curve by differential evolution (Black line), and estimated AIF (green line), summed kinetics of the two peaks (blue line) from the Left (B) and Right (C) foot. The number within the graph indicates perfusion rate.